

Selective Excitation of Ti^{2+} Dimers and Trimers in $MgCl_2$ Markus Herren, Stuart M. Jacobsen,[†] and Hans U. Güdel*

Received July 27, 1990

The low-temperature near-infrared (near-IR) luminescence spectrum of $MgCl_2:2\% Ti^{2+}$ consists of a series of sharp lines, which can be clearly assigned to Ti^{2+} single ions, dimers, and trimers. With laser excitation into a $Ti^{2+}Ti^{2+}$ double absorption (${}^3A_{2g}{}^3A_{2g} \rightarrow {}^1E_g{}^1A_{1g} (D_{3d})$) at 24040 cm^{-1} , dimer and trimer near-IR-luminescence lines are selectively obtained. The intensity of the observed cluster transitions is due to an exchange mechanism. The coupling is antiferromagnetic, and the exchange parameter $-2J$ between nearest-neighbor Ti^{2+} ions is estimated to be greater than 100 cm^{-1} . The temperature dependence of the most intense dimer near-IR-luminescence lines is explained by spin-orbit splitting in the ground and excited states.

1. Introduction

Exchange interactions in dimers and trimers of transition-metal ions have been extensively studied over the past twenty years. They serve as simple molecular models for the magnetically ordered systems with extended interactions. In many cases correlations were established between the low-temperature magnetic properties and the structure.^{1a} Optical spectroscopic techniques have played a complementary role in this research to the more widely used magnetochemical methods.^{1b,2} Absorption and luminescence spectroscopy were found to be particularly useful in the study of exchange-coupled Cr^{3+} clusters.²

The Ti^{2+} ion is by far the least studied among the divalent 3d transition-metal ions. It is not stable in aqueous solution, but some crystalline halide compounds such as $TiCl_2$, $TiBr_2$, TiI_2 , $RbTiCl_3$, and $CsTiCl_3$ have been synthesized.^{3,4} Recently, Morita et al. reported a high-pressure synthesis for the so far unknown TiF_2 .⁵ Magnetic measurements on $TiCl_2$ were interpreted in terms of very strong antiferromagnetic $Ti^{2+}-Ti^{2+}$ exchange interactions.⁶

Exchange-coupled dimers and trimers of Ti^{2+} have not been studied before. Ti^{2+} can be doped into ionic halide lattices,⁷ and several optical spectroscopic studies of Ti^{2+} single ions in $MgCl_2$ have recently been published.⁸⁻¹⁰ In this lattice, Ti^{2+} shows at low temperature a near-infrared (near-IR) luminescence spectrum consisting of a series of sharp lines, most of them being electronic origins. Since the emitting state ${}^1E_g (D_{3d})$ is not split, the near-IR luminescence spectrum shows directly the ground-state splitting pattern. In a previous study, we investigated exchange splittings of $Ti^{2+}Mn^{2+}$ dimers and $Mn^{2+}Ti^{2+}Mn^{2+}$ trimers in $MgCl_2$ by selective laser excitation.^{11,12} In $MgCl_2:2\% Ti^{2+}$, the crystals studied in the present work, only 11% of the Ti^{2+} ions belong to clusters, and single ions dominate the luminescence spectrum upon unselective excitation. Tunable laser spectroscopy is therefore also used in this study to selectively excite and investigate Ti^{2+} dimers and trimers.

$MgCl_2$ possesses a layer lattice with the $CdCl_2$ structure, space group $R\bar{3}m$.¹³ Each Mg^{2+} ion has six nearest neighbors of Mg^{2+} , all lying in one plane. Part of a Mg^{2+} layer is drawn in Figure 1. Neighboring Mg^{2+} ions are bridged by two Cl^- ions, which lie above and below the plane, respectively. Besides the single ions all the relevant Ti^{2+} species with nearest-neighbor exchange are shown (dimer, linear and bent trimer chain, triangular trimer).

2. Experimental Section

Single crystals of $MgCl_2$ containing Ti^{2+} were grown by the Bridgman technique, as described in ref 8. Titanium metal was oxidized by Zn^{2+} in the magnesium chloride melt at $800\text{ }^\circ\text{C}$. The crystals are green and cleave easily parallel to the crystallographic layers. The titanium concentration was determined colorimetrically by forming a yellow aqueous peroxy complex.¹⁴ To get a crystal with 2% Ti^{2+} , a nominal dopant concentration of 5% was used. All experiments in the present study were carried out on thin platelets in an axial configuration.

In the selective experiments luminescence was excited by a tunable Lambda Physik FL3002 dye laser with Stilbene 3, pumped by the third

harmonic (355 nm) of a pulsed Quanta-Ray DCR-3D Nd:YAG laser. In survey experiments light of a halogen or a xenon lamp was used, filtered by a $1/4\text{-m}$ monochromator or a combination of a $CuSO_4$ solution with glass and interference filters, depending on the wavelength range. Luminescence was dispersed by a $3/4\text{-m}$ Spex 1702 monochromator and detected by a cooled (77 K) germanium photodetector (Applied Detector Corp. 403L). Cooling of the sample was achieved either with helium gas in a silica flow tube¹⁵ or, for $T \leq 4.2\text{ K}$, a liquid-helium-bath cryostat (Oxford Instruments MD4). Absorption spectra were obtained on a Cary 17 spectrometer with an Air Products closed-cycle helium refrigerator for sample cooling.

3. Results

3.1. Unselective Excitation of Ti^{2+} into ${}^3T_{2g} (O_h)$. The low-temperature near-IR luminescence spectrum of Ti^{2+} single ions in $MgCl_2$ consists of two series of lines, corresponding to the transitions from the first excited state ${}^1E_g (D_{3d})$ to the two trigonal components ${}^3A_{2g}$ and ${}^3E_g (D_{3d})$ of the ${}^3T_{1g} (O_h)$ ground state.⁸ Figure 2A shows the spectrum for $MgCl_2:0.05\% Ti^{2+}$ with the assignment of sharp electronic origins and broader vibronic features. Excitation was made into the ${}^3T_{2g} (O_h)$ spin-allowed absorption band in the near-IR region. By use of the same excitation for a crystal with 2% Ti^{2+} , new lines are observed; see Figure 2B.¹⁶ They can be assigned to dimers (D) and trimers ($T_{1,2,3}$) from their concentration dependence, as indicated in Figure 2. Most of the intensity of the dimer and trimer luminescence is concentrated in the ${}^3A_{2g}$ origin region around 7500 cm^{-1} ; vibronic sidebands are missing. All the D and T lines are found at energies lower than those of the corresponding single-ion lines. No cluster lines are detected in the 3E_g region around 6900 cm^{-1} . A new group of lines is observed, however, near 6100 cm^{-1} . There are no transitions in the single-ion spectrum of Ti^{2+} in this spectral region, and we can readily assign them to dimer transitions. Since the energy difference to the ${}^3A_{2g}{}^3A_{2g}$ dimer origins at 7550 cm^{-1} is

- (1) (a) *Magneto-Structural Correlations in Exchange Coupled Systems*; Willett, R. D., Gatteschi, D., Kahn, O., Eds.; Reidel: Dordrecht, The Netherlands, 1985. (b) Güdel, H. U. In ref 1a, pp 297-327.
- (2) McCarthy, P. J.; Güdel, H. U. *Coord. Chem. Rev.* **1988**, *88*, 69.
- (3) Klemm, W.; Grimm, L. *Z. Anorg. Allg. Chem.* **1942**, *249*, 198.
- (4) Meyer, G.; Packruhn, U. *Z. Anorg. Allg. Chem.* **1985**, *524*, 90.
- (5) Morita, N.; Endo, T.; Sato, T.; Shimada, M. *J. Mater. Sci. Lett.* **1987**, *6*, 859.
- (6) Klemm, W.; Grimm, L. *Z. Anorg. Allg. Chem.* **1942**, *249*, 209.
- (7) Wilson, D. R.; Brown, D. H.; Smith, W. E. *Inorg. Chem.* **1986**, *25*, 898.
- (8) Jacobsen, S. M.; Güdel, H. U.; Daul, C. A. *J. Am. Chem. Soc.* **1988**, *110*, 7610.
- (9) Jacobsen, S. M.; Güdel, H. U. *J. Lumin.* **1989**, *43*, 125.
- (10) Jacobsen, S. M.; Güdel, H. U.; Daul, C. A. *Chem. Phys. Lett.* **1989**, *158*, 77.
- (11) Herren, M.; Jacobsen, S. M.; Güdel, H. U. *Inorg. Chem.* **1989**, *28*, 504.
- (12) Herren, M.; Jacobsen, S. M.; Güdel, H. U.; Briat, B. *J. Chem. Phys.* **1989**, *90*, 663.
- (13) Wyckoff, R. W. G. *Crystal Structures*, 2nd ed.; Interscience: New York, 1965; Vol. 1, p 270.
- (14) Cotton, F. A.; Wilkinson, G. *Advanced Inorganic Chemistry*; Interscience: New York, 1962; p 670.
- (15) Krausz, E.; Tomkins, C.; Adler, H. *J. Phys. E* **1982**, *15*, 1167.
- (16) Jacobsen, S. M.; Herren, M.; Güdel, H. U. *J. Lumin.* **1990**, *45*, 369.

* To whom correspondence should be addressed.

[†] Present address: Department of Physics and Astronomy, University of Georgia, Athens, GA 30602.

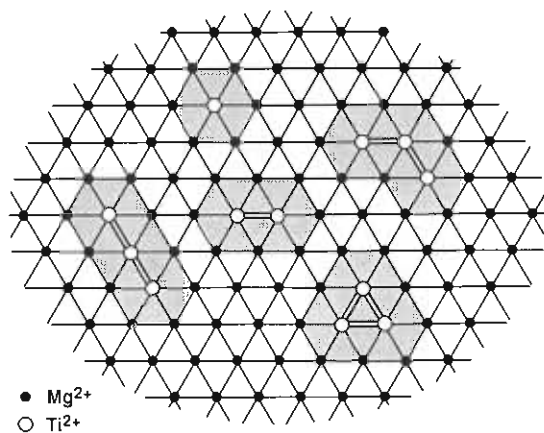


Figure 1. Layer of $\text{MgCl}_2 \cdot 2\text{Ti}^{2+}$. Only the metal ions are drawn. The shaded areas mark the Ti^{2+} species investigated in the present study. Exchange-coupled Ti^{2+} ions are connected by bold lines.

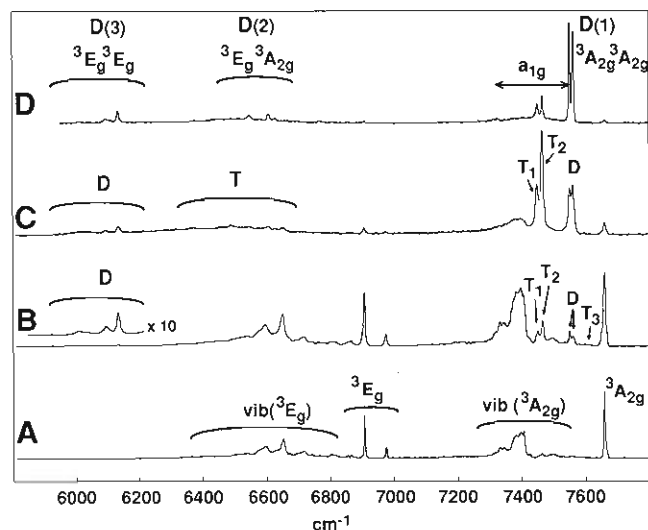


Figure 2. Low-temperature near-infrared (near-IR) luminescence spectra of $\text{MgCl}_2 \cdot 2\text{Ti}^{2+}$ with different excitation. Dimer lines are marked D(1), D(2), and D(3), referring to the transitions indicated in Figure 7. Trimer lines are marked T_1 , T_2 , and T_3 , indicating linear chains, bent chains, and triangles, respectively. Key: (A) 0.05% Ti^{2+} , 6 K, excitation at 9000–11 000 cm^{-1} (from ref 8); (B) 2% Ti^{2+} , 6 K, excitation at 9000–11 000 cm^{-1} (from ref 16); (C) 2% Ti^{2+} , 15 K, excitation at 20 000–30 000 cm^{-1} ; (D) 2% Ti^{2+} , 16 K, excitation at 24 040 cm^{-1} .

twice the trigonal ground-state splitting of a Ti^{2+} single ion, this new low-energy luminescence is assigned to transitions in which both ions of a dimer end up in the higher trigonal component of the ground state: 3E_g ; see Figure 2 and section 4.3. With unselective Ti^{2+} excitation of a 2% crystal no other dimer or trimer lines can be identified in the luminescence spectrum.

3.2. Selective Cluster Excitation. In the absorption spectrum of $\text{MgCl}_2 \cdot 2\text{Ti}^{2+}$ a sharp band, centered at 24 040 cm^{-1} , with an extinction coefficient $\epsilon = 4$ is observed, which is missing in more diluted crystals⁸ and therefore assigned to a Ti^{2+} cluster absorption. When the crystal is excited in this energy region, new intensity ratios in the near-IR luminescence spectrum are obtained; see Figure 2C,D. Most of the luminescence intensity now lies in the D and T lines. Two different excitation sources were used: (i) a filtered xenon lamp with blue (20 000–30 000 cm^{-1}) broadband light (Figure 2C) and (ii) a dye laser at 24 040 cm^{-1} (Figure 2D). In both luminescence spectra there is a very small contribution from Ti^{2+} single ions, because the broad ${}^3A_{2g}$ two-electron transition, centered at 19 300 cm^{-1} , has some intensity up to 24 040 cm^{-1} .⁸ Selective excitation spectra were run for the dimer and trimer emissions. They show a great deal of overlap, all peaking at about 24 040 cm^{-1} , with widths of approximately 100, 300, and 500 cm^{-1} for lines D, T_1 , and T_2 , respectively. Broad-band blue

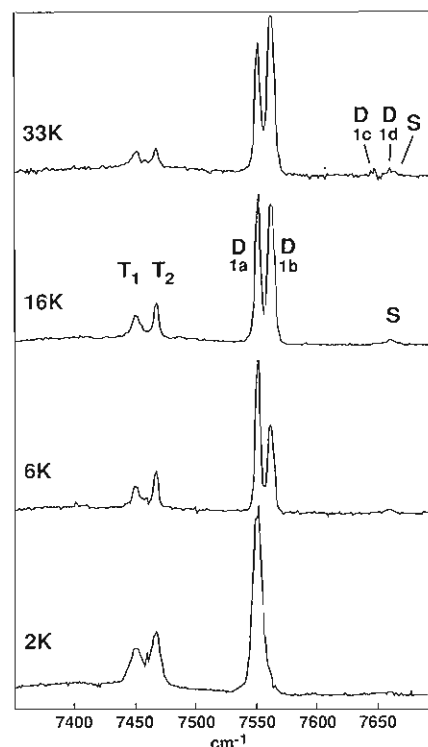


Figure 3. High-energy origin region of the near-IR luminescence spectrum of $\text{MgCl}_2 \cdot 2\text{Ti}^{2+}$, excited at 24 040 cm^{-1} , for four temperatures. S, D, and T mark single-ion, dimer, and trimer lines, respectively.

light thus favors trimer excitation compared to 24 040- cm^{-1} laser light; cf. Figure 2C,D.

Since virtually no Ti^{2+} single ions are excited at 24 040 cm^{-1} , this absorption has to be assigned to a transition in which two Ti^{2+} ions are simultaneously excited, i.e. a double excitation.² This will be discussed in section 4.2. Although Ti^{2+} dimer (D) and two types of trimer emission lines (T_1 , T_2) are enhanced by exciting with blue light, no measurable intensity is observed for the trimer line T_3 at 7600 cm^{-1} . It is different from the other two trimer lines in intensity and energy position and by this argument assigned to Ti^{2+} triangles, which are expected to be clearly distinguishable from trimer chains. Considering statistical abundances (1:2 for the linear:bent chain ratio), T_1 and T_2 can be assigned as shown in Figure 2B,C. It is theoretically expected (see section 4.2) that the double excitation at 24 040 cm^{-1} is only efficient for Ti^{2+} trimer chains but not for triangles at low temperature.

The luminescence spectra obtained with selective excitation reveal some features that were not observed before: (i) a broad, structured emission band between 6200 and 6600 cm^{-1} due to trimers (Figure 2C) and (ii) some sharp lines between 6500 and 6650 cm^{-1} due to dimers (Figure 2D). In addition, two weak dimer lines at 7315 and 7326 cm^{-1} are found and assigned to an a_{1g} vibrational sideband of the electronic origins at 7551 and 7562 cm^{-1} . The same value of 236 cm^{-1} for the totally symmetric mode was measured for $\text{Ti}^{2+}\text{Mn}^{2+}$ dimers in MgCl_2 .¹¹ For Ti^{2+} single ions this mode has a frequency of 260 cm^{-1} .⁸

3.3. Temperature Dependence of ${}^3A_{2g}$ Dimer Emission Lines. In Figure 3 the ${}^3A_{2g}$ region of the dimer luminescence spectrum is shown at four different temperatures. The intensity ratio of the lines 1a (cold) and 1b (hot) is strongly temperature dependent, whereas the total intensity of these two lines is essentially unaffected by temperature variation between 2 and 33 K. In Figure 4 the temperature dependence of the 1a intensity is shown and related to a model discussed in section 4.3.

At 33 K two hot dimer lines at 7646 (1c) and 7657 cm^{-1} (1d) are just barely observed; see Figure 3. One of them is partially overlapping with the temperature-independent single-ion line. The energy separation from the two prominent dimer lines 1a and 1b is 95 cm^{-1} .

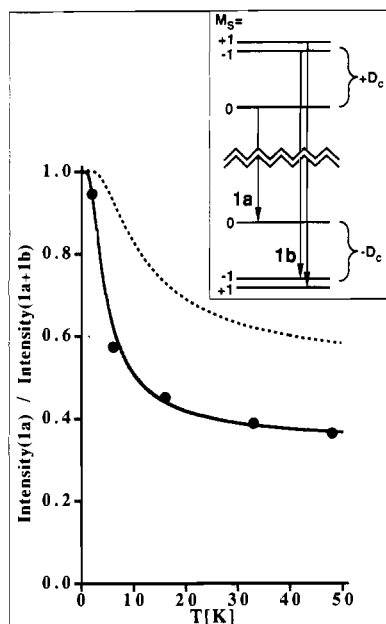


Figure 4. Temperature dependence of the intensity ratio $I_a/(I_a + I_b)$. Points indicate experimental values. The solid line is calculated with the model in the insert for $D_c = 5 \text{ cm}^{-1}$. The broken line is calculated for an 11-cm^{-1} orbital splitting in the emitting state (see section 4.3.). Insert: Zero-field splitting of the emitting state and lowest triplet level of the ground state, with the approximations of section 4.3. Arrows indicate transitions that are allowed by the exchange mechanism.

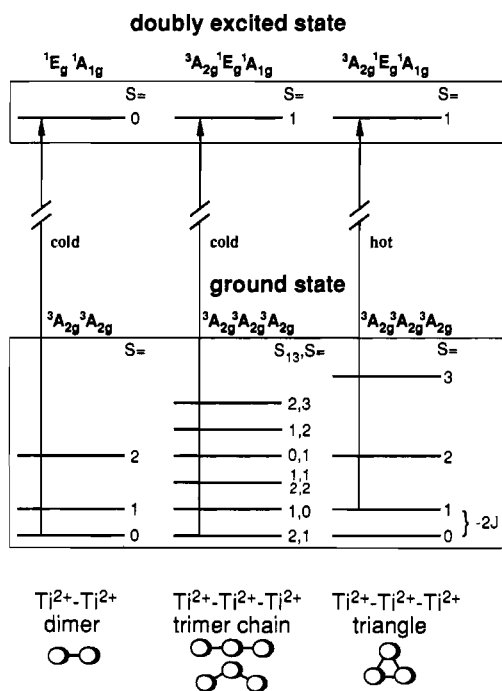


Figure 5. Ground state and doubly excited state of Ti^{2+} dimers, trimer chains, and triangles. Arrows mark the allowed double excitations.

4. Analysis and Discussion

4.1. Ground State of Ti^{2+} Dimers and Trimers. The Ti^{2+} single ion in MgCl_2 has a ${}^3A_{2g}$ ground state with $g = 1.99$.¹⁰ The exchange interactions between two Ti^{2+} ions can thus simply be described by a Heisenberg operator:

$$\hat{H}_{\text{ex}} = -2J(\mathbf{S}_1 \cdot \mathbf{S}_2) \quad (1)$$

With $S_1 = S_2 = 1$ the result is a Landé splitting pattern with energy levels

$$E(S) = -J[S(S + 1) - 4] \quad (2)$$

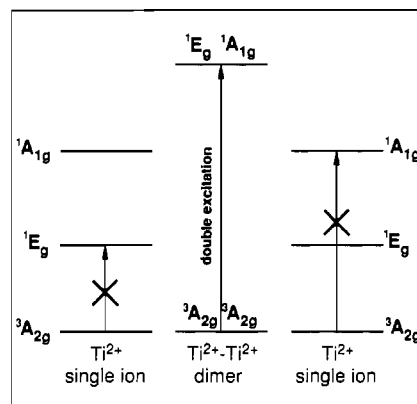


Figure 6. Schematic representation of the observed double excitation in a dimer.

where S is the total dimer spin ($S = 0, 1, 2$); see bottom of Figure 5.

For an equilateral Ti^{2+} triangle the operator is given by

$$\hat{H}_{\text{ex}} = -2J(\mathbf{S}_1 \cdot \mathbf{S}_2 + \mathbf{S}_2 \cdot \mathbf{S}_3 + \mathbf{S}_3 \cdot \mathbf{S}_1) \quad (3)$$

which also leads to a Landé splitting pattern with

$$E(S) = -J[S(S + 1) - 6] \quad (4)$$

and $S = 0, 1, 2$, and 3 ; see bottom of Figure 5. The degeneracies of the four levels are 1, 9, 10, and 7, respectively.

The situation is different for Ti^{2+} trimer chains, in which exchange interactions between the two terminal ions may be neglected in a first approximation:

$$\hat{H}_{\text{ex}} = -2J(\mathbf{S}_1 \cdot \mathbf{S}_2 + \mathbf{S}_2 \cdot \mathbf{S}_3) \quad (5)$$

In this case the central ion (2) takes a special position and the energy levels have to be described by two quantum numbers: $S_{13} = 0, 1$, and 2 and the total trimer spin $S = 0, 1, 2$, and 3 . The energy levels are given by

$$E(S_{13}, S) = -J[S(S + 1) - S_{13}(S_{13} + 1) - 2] \quad (6)$$

which leads to a splitting pattern with equidistant energy levels. This pattern is also shown in the lower part of Figure 5. All splitting patterns are shown for negative values of J , i.e. antiferromagnetic coupling, because this is the only way to relate them to our experimental results.

4.2. Double Excitation. The sharp absorption band centered at 24040 cm^{-1} (see section 3.2) is assigned to a transition involving the simultaneous excitation of two exchange-coupled Ti^{2+} ions. From the sharpness of the band we conclude that both excitations occur within the electron configuration of the ground state. These transitions are extremely weak in the single ion, and none has been observed in the absorption spectrum so far. However, the position of the first excited-state 1E_g (D_{3d}) in Ti^{2+} single ions is exactly known from the luminescence spectrum (7665 cm^{-1}),⁸ and the ${}^3A_{2g} \leftrightarrow {}^1A_{1g}$ transition energy is known from an excited-state excitation experiment (16200 cm^{-1}).⁹ The sum of both transition energies is 23865 cm^{-1} , very close to the 24040-cm^{-1} cluster absorption line. We thus assign this line to a ${}^3A_{2g} {}^3A_{2g} \rightarrow {}^1A_{1g} {}^1E_g$ double excitation in both dimers and trimers. The mismatch in energy is explained by slightly different electron repulsion parameters for single ions and clusters and by the cluster ground-state stabilization due to exchange interactions ($-4J$ for dimers and $-6J$ for trimers, according to eqs 2, 4, and 6).

Figure 6 shows a schematic representation of the transitions involved in the double excitation. Both single-ion excitations ${}^3A_{2g} \rightarrow {}^1A_{1g}$ and ${}^3A_{2g} \rightarrow {}^1E_g$ are spin-forbidden, but occurring simultaneously in a cluster, they combine to an allowed transition, gaining its intensity by an exchange mechanism.² The doubly excited state is shown in Figure 5 for Ti^{2+} dimers and trimers. It is not split by exchange, since no exchange interaction is possible with ions in singlet states. A small splitting due to the removal of the orbital degeneracy of 1E_g in the lower than D_{3d} point

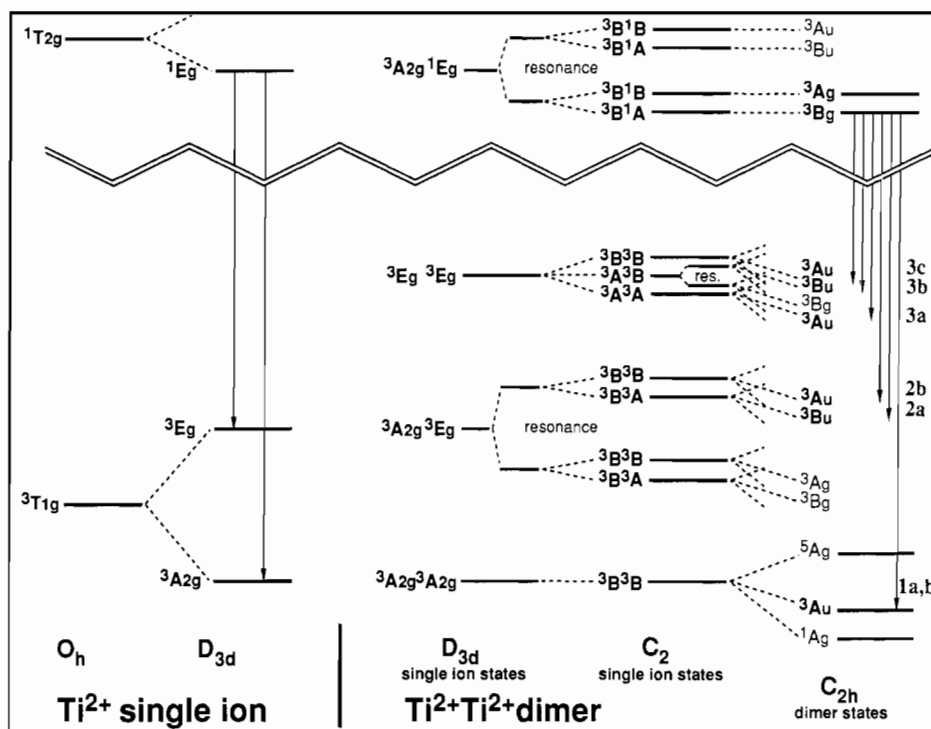


Figure 7. Energy splittings of Ti^{2+} single ions and dimers, as discussed in section 4.3. The effects of symmetry lowering and exchange interactions are shown, but spin-orbit coupling is neglected. Arrows indicate the allowed transitions for single ions and dimers at low temperature.

symmetry as well as a possible resonance splitting can be neglected here, because they are experimentally not accessible. The exchange mechanism requires the selection rule $\Delta S = 0$,¹⁷ so that double excitations are allowed, at low temperature, for Ti^{2+} dimers and trimer chains but not for triangles (see Figure 5). The only allowed transition in the triangular trimer is hot, originating in the first excited trimer level $S = 1$. This is in very nice agreement with our failure to excite triangles up to 50 K with broad-band blue light. From this we estimate a lower limit for the singlet-triplet energy separation ($-2J$) in triangular trimers of 100 cm^{-1} .

4.3. Emission from Ti^{2+} Dimers. In order to understand the spectral differences between single-ion and dimer luminescence, we refer to Figure 7, in which the relevant splittings and transitions are schematically shown. Dimer states are derived from single-ion states⁸ by considering consecutively the lowering of the Ti^{2+} point symmetry and exchange interactions. In this overview spin-orbit coupling effects are neglected. The trigonal ground-state splitting leads to three distinct dimer configurations: (i) both ions in $3A_{2g}$, (ii) one ion in $3A_{2g}$ and one in $3E_g$ (singly excited ground state), and (iii) both ions in $3E_g$ (doubly excited ground state). For the singly excited ground state and for the excited state we have to consider resonance between the equivalent localized combinations $3A_{2g}\Gamma$ and Γ^3A_{2g} ($\Gamma = 3E_g$ and $3E_g$, respectively). A nonzero excitation-transfer integral of the form¹⁷

$$H_{ET} = \langle 3A_{2g}\Gamma | \hat{H}_{ex} | \Gamma^3A_{2g} \rangle \quad (7)$$

leads to an additional energy splitting of $2H_{ET}$. And the proper pair wave functions are given by

$$\Psi_{\pm} = 1/\sqrt{2}(|3A_{2g}\Gamma\rangle \pm |\Gamma^3A_{2g}\rangle) \quad (8)$$

The site symmetry of a Ti^{2+} ion in MgCl_2 is D_{3d} if it is a single ion but only C_2 if it is a member of a dimer. In addition to the trigonal crystal field there is thus a small rhombic component, which can lead to an additional orbital splitting; see Figure 7. The important step is now the combination of C_2 single-ion states to C_{2h} dimer states; see the last column of Figure 7. In all the ground-state components there is a set of spin singlet, triplet, and quintet levels, as shown for $3A_{2g}3A_{2g}$. For the higher energy states

only the spin triplets are labeled in Figure 7 for clarity. In the emitting state there is no exchange interaction and therefore $S = 1$. Low-temperature transitions allowed by parity and the spin selection rule $\Delta S = 0$ are indicated by arrows.

We can now discuss the observed dimer spectrum of Figure 2D in terms of this model. It mainly consists of electronic origins, and the intense vibronic features, typical for single ions, are not observed. This difference is explained by the different intensity mechanisms in single ions and dimers. Whereas electronic origins can only have magnetic dipole intensity in isolated single ions (D_{3d} site symmetry), they can gain electric dipole intensity by an exchange mechanism in dimers.¹⁷ The only vibrational sidebands in the dimer spectrum correspond to the totally symmetrical a_{1g} mode, and they are weak. The luminescence spectrum can thus directly be correlated with the predicted pattern of spectroscopically accessible dimer ground-state levels in Figure 7. The two most intense dimer lines lying at the highest energy are assigned to transitions 1a,b. They appear 100 cm^{-1} at lower energy than the single-ion origin, since the electron repulsion parameters are smaller in clusters due to stronger delocalization of the unpaired electrons. Almost 1000 cm^{-1} to lower energy there is a group of lines corresponding to 2a,b. The spectral position confirms the predicted sign of the $3A_{2g}3E_g$ resonance splitting given for antiferromagnetic coupling. The dimer luminescence lines below 6200 cm^{-1} are assigned to transitions (3a-c) to the high-lying $3E_g3E_g$ dimer ground-state configuration, which has obviously no single-ion counterpart; see Figure 7. The existence of these dimer lines at lower energy than all the single-ion lines is thus theoretically well explained. A detailed analysis of the $3A_{2g}3E_g$ and $3E_g3E_g$ regions cannot be given, since the zero-field splittings of these states are not easily estimated and there are too many parameters (zero-field, rhombic and resonance splittings). However, the predictions in Figure 7 are in good overall agreement with the dimer luminescence spectrum in Figure 2D.

Line 1 is observed to be split by 11 cm^{-1} into two components 1a and 1b. The temperature dependence of these two lines (see Figure 3) is the result of a splitting in the emitting state. A quantitative analysis reveals that it is not, as one might expect, due to a rhombic splitting of 11 cm^{-1} between $3B_g$ and $3A_g$ (cf. the broken line in Figure 4). We have to postulate an additional splitting of the lower $3B_g$ component due to second-order spin-orbit coupling. As shown in Figure 4, the measured temperature de-

(17) Ferguson, J.; Guggenheim, H. J.; Tanabe, Y. *J. Phys. Soc. Jpn.* **1966**, *21*, 692.

pendence is exactly reproduced with a zero-field splitting (ZFS) of 3B_g by 5 cm^{-1} . This splitting is correlated with the ZFS in the ground state as follows. In a Ti^{2+} single ion the ${}^3A_{2g}$ ground state has a ZFS $D_c = 4.7\text{ cm}^{-1}$ into an A_{1g} (lower) and an E_g (higher) spinor component (D_{3d}).⁸ In the dimer this zero-field splitting now occurs in the excited-state ${}^3A_{2g}^1E_g$, giving rise to the observed temperature dependence. In the dimer ground-state ${}^3A_{2g}^3A_{2g}$ the ZFS of the $S = 1$ level D_1 can be correlated with the single-ion value D_c by the following formula:¹⁸

$$D_1 = -D_c + 3D_e \quad (9)$$

where D_e arises from anisotropic exchange and dipole-dipole interactions. In an exchange-coupled dimer of Cr^{3+} , D_e was found to provide a negligible correction for D_c .¹⁹ Assuming the same to be true here, the ZFS in the $S = 1$ dimer ground state has thus approximately the same value as in the dimer excited state but with opposite sign. This is indeed borne out by our experiments. As a result of the $\Delta M_S = 0$ selection rule for an exchange mechanism, only two transitions are allowed, with an energy difference of $|D_1| + |D_c| = 10\text{ cm}^{-1}$; see Figure 4. The observed 11-cm^{-1} splitting of the dimer emission lines 1a and 1b is in excellent agreement with this.

The hot lines 1c and 1d in the 33 K spectrum of Figure 3 are assigned to transitions from the higher rhombic component of the *gerade* emitting state to the 3A_u ground state. The temperature dependence is consistent with an excited-state splitting of 95 cm^{-1} , corresponding to the energy separation between 1a,b and 1c,d. The ${}^3A_g^3B_g$ splitting is thus considerably larger than the corresponding splitting of 12.5 cm^{-1} in $\text{Ti}^{2+}\text{Mn}^{2+}$ dimers.¹¹ We attribute this difference to the larger ionic radius of Ti^{2+} causing a stronger lattice distortion. In addition the higher covalency within Ti-Cl-Ti may contribute to this splitting.

No transitions to the singlet and quintet levels of the ${}^3A_{2g}^3A_{2g}$ ground state are observed. This is in contrast to $\text{Ti}^{2+}\text{Mn}^{2+}$ dimers in MgCl_2 ¹¹ and to all the systems of exchange-coupled Cr^{3+} ions that have been studied by optical spectroscopy. We are therefore unable to directly determine the exchange splitting of the Ti^{2+} dimer ground state by optical spectroscopy. The fact that the $\Delta S = \pm 1$ dimer transitions are at least 2 orders of magnitude weaker than the $\Delta S = 0$ transitions is in good agreement with our conclusion that the antiferromagnetic coupling is very strong ($-2J \geq 100\text{ cm}^{-1}$ in the triangular trimers). The Tanabe intensity mechanism is absolutely dominant for the dimer and trimer

transition, and a careful examination of this mechanism shows that both the exchange parameters J and the intensity coefficients Π derive their strength from the same one-electron-transfer integrals.²⁰ This can in turn be correlated with the covalency of the $\text{M}^{2+}\text{-Cl}^-$ bond, which is stronger for $\text{Ti}^{2+}\text{-Cl}^-$ than for any other divalent 3d transition-metal ion. TiCl_2 is black, indicating a rather low-lying conduction band, whereas all the other chlorides of divalent 3d ions are transparent. Small values of both the molar volume³ and the magnetic susceptibility⁶ of TiCl_2 reflect the high covalency of the Ti-Cl-Ti bonds and thus the strongly antiferromagnetic $\text{Ti}^{2+}\text{-Ti}^{2+}$ exchange interaction.

4.4. Emission from Ti^{2+} Trimers. The most intense luminescence lines of linear and bent trimer chains are T_1 and T_2 at 7450 and 7467 cm^{-1} , respectively. They correspond to transitions to the ${}^3A_{2g}^3A_{2g}^3A_{2g}$ ground-state configuration. As shown in the lower part of Figure 5, there is only one ground-state level with $S = 0$, in contrast to the numerous $S = 1$ and $S = 2$ levels. Since only one line for each species is observed, we conclude that the emission is due to a transition from an $S = 0$ level of the ${}^3A_{2g}^3A_{2g}^1E_g$ singly excited state to the $|1,0\rangle$ ground-state level. The exchange splitting pattern of ${}^3A_{2g}^3A_{2g}^1E_g$ is expected to correspond to the ${}^3A_{2g}^3A_{2g}$ dimer ground-state splitting, the lowest level having $S = 0$. In contrast to the dimer emission lines, the trimer emission lines are not split by a second-order spin-orbit interaction. This nicely confirms their assignment to $S = 0 \rightarrow S = 0$ transitions.

The features around 6500 cm^{-1} in Figure 2C are assigned to transitions to the singly excited trimer ground state ${}^3A_{2g}^3A_{2g}^3E_g$. As in the dimers, there is a resonance splitting of this state, and we only observe transitions to one component. All other trimer transitions are assumed to occur at energies below 6000 cm^{-1} , which is out of range of the near-IR detector used in this study. In contrast to dimers there is a resonance splitting of the ${}^3A_{2g}^3E_g^3E_g$ doubly excited trimer ground state, which explains the absence of trimer lines around 6100 cm^{-1} . Transitions to the triply excited trimer ground states ${}^3E_g^3E_g^3E_g$ are expected to occur around 5250 cm^{-1} .

All trimer lines are shifted by about 100 cm^{-1} to lower energy relative to the corresponding dimer lines, due to smaller electron repulsion parameters. This is the result of increasing delocalization of the unpaired electrons, going from single ions to dimers to trimers.

Acknowledgment. This work was financially supported by the Swiss National Science Foundation.

(18) Owen, J.; Harris, E. A. *Electron Paramagnetic Resonance*; Geschwind, S., Ed.; Plenum Press: New York, 1972; p 446.

(19) Riesen, H.; Güdel, H. U. *Mol. Phys.* **1987**, *60*, 1221.

(20) Gondaira, K.; Tanabe, Y. *J. Phys. Soc. Jpn.* **1966**, *21*, 1527.

Notes

Contribution from the Research School of Chemistry,
The Australian National University, G.P.O. Box 4,
Canberra, ACT 2601, Australia

Metal-Metal Bonds in Tl(I)-Tl(I) Compounds: Fact or Fiction?

Peter Schwerdtfeger

Received August 6, 1990

Until recently, Tl-Tl interactions have been generally regarded as weak and have been postulated on the basis of vibrational and X-ray measurements on some inorganic Tl(I) compounds.^{1,2} In

contrast, element-element bonds in inorganic and organometallic compounds of B, Al, Ga, and In are well-known. However, Schumann and co-workers³ recently obtained (η^5 -pentabenzylcyclopentadienyl)thallium(I), (η^5 -($\text{C}_6\text{H}_5\text{CH}_2$)₅C₅)Tl, in dimeric form in the solid state with a Tl-Tl distance of 3.632 \AA and a ring-center-Tl1-Tl2 angle α of 131.8° . Most CpTl derivatives crystallize in polymeric zigzag chains, containing alternating Tl atoms and Cp rings. Schumann et al. concluded that the distance between the two thallium atoms is far too large for a conventional metal-to-metal bond. Moreover, the CpM compounds ($M = \text{In}, \text{Tl}$) so far studied are monomeric in solution, which suggests that the interaction is weak. However, Janiak and Hoffmann⁴ have

(1) Taylor, M. J. *Metal-to-Metal Bonded States of the Main Group Elements*; Academic: London 1975.

(2) Schwerdtfeger, P.; Boyd, P. D. W.; Bowmaker, G. A.; Mack, H. G.; Oberhammer, H. *J. Am. Chem. Soc.* **1989**, *111*, 15.

(3) Schumann, H.; Janiak, C.; Pickardt, J.; Börner, U. *Angew. Chem.* **1987**, *99*, 788; *Angew. Chem., Int. Ed. Engl.* **1987**, *26*, 789.

(4) (a) Janiak, C.; Hoffmann, R. *Angew. Chem.* **1989**, *101*, 1706; *Angew. Chem., Int. Ed. Engl.* **1989**, *28*, 1688. (b) Janiak, C.; Hoffmann, R. *J. Am. Chem. Soc.* **1990**, *112*, 5924.